NEP Estimation of Terrestrial Ecosystems in China Using an Improved CASA Model and Soil Respiration Model

Liang Liang, Qianjie Wang, Siyi Qiu, Di Geng, and Shuguo Wang

***Abstract*—Net ecosystem productivity (NEP) is a critical indicator of the CO_2 capture capacity of vegetation ecosystems. Based on the land classification and clumping index (CI) datasets, the key parameters of the Carnegie–Ames–Stanford Approach (CASA) model, including fraction of photosynthetic active radiation (FPAR) and maximum light use efficiency (ε_{max}), were optimized. Then, the NEP of China's terrestrial ecosystems was estimated, using the improved CASA coupled with a soil respiration model. Finally, the accuracy of NEP estimation was evaluated by observation data from ChinaFLUX station. The research results indicated the RMSE of the improved NEP estimations decreased from 21.139 to 10.179 (unit: $gC \cdot m^{-2} \cdot month^{-1}$), and the R^2 value increased from 0.413 to 0.832, indicating that optimizing the parameters ε_{max} and FPAR are both effective methods to improve the model. The spatiotemporal variation of China's NEP was analyzed using the optimized results. The NEP value of China shows a decreasing distribution pattern from southeast to northwest, and the values of different regions are in the order South > North > Qinghai–Tibet > Northwest. The monthly NEP variation in different regions of China is a unimodal curve, reaching the maximum in summer. This study optimized the NEP estimation, which can better characterize the distribution pattern of carbon sinks/sources in China's terrestrial ecosystems and lay a scientific foundation for developing regional carbon neutrality schemes.**

***Index Terms*—Carbon sink, Carnegie–Ames–Stanford Approach (CASA) model, clumping index (CI), light use efficiency (LUE), Net ecosystem productivity (NEP), NPP.**

I. Introduction

NET ecosystem productivity (NEP) is a critical indicator, which can represent the actual carbon sequestration capacity of ecosystems [1]. A positive NEP indicates the ecosystem generally absorbs CO_2, which is a carbon sink; In contrast, a minus value represents the ecosystem generally releases CO_2 and is a carbon source. China is a country with a vast territory and high ecosystem diversity. Thus, it is necessary to accurately obtain the terrestrial NEP values to assess the carbon sink capacity of Chinese ecosystems and formulate appropriate carbon neutralization schemes [2], [3].

The NEP value is calculated from net primary productivity (NPP) minus soil heterotrophic respiration (R_h), i.e., NEP = NPP-R_h [4]. Traditional methods for obtaining NPP include the biomass survey, direct harvest, and eddy covariance correlation [5]. These methods can obtain NEP values accurately, however, they are labor-intensive and time-consuming, and are point-source data, so it is difficult to estimate NPP at the large scale. Therefore, on the large scale, NPP is mainly estimated by models [6], [7]. At present, the models used for NPP estimation include light use efficiency (LUE) model, climate model, and process model [7]. The Carnegie–Ames–Stanford Approach (CASA) LUE model is practical and simple and can fully utilize a variety of remote sensing data to obtain NPP on a large scale regularly and frequently [7], [8]. Therefore, it is favored by researchers and has become one of the most popular models to estimate NPP at the large scale.

The CASA model uses the absorbed photosynthetically active radiation (APAR) determined by vegetation characteristics and real LUE ($\varepsilon(x, t)$) limited by environmental factors to characterize NPP. $\varepsilon(x, t)$ is limited by environmental variables such as humidity and temperature, as well as related to the maximum LUE (ε_{max}) of vegetation. Initially, ε_{max} was defined as a fixed value ($0.389\ gC \cdot MJ^{-1}$) [6], [9]. However, because the photosynthetic capacity of various types of vegetation is different, it is more reasonable to set ε_{max} based on the type of vegetation. In this work, according to previous studies on the ε_{max} of various vegetation types and on the land cover classification data, the ε_{max} values were optimized to improve the model [10], [11].

In addition, the model uses the parameter fraction of photosynthetically active radiation (FPAR), which is the main variable to characterize the APAR, to describe the light energy interception ability of the vegetation canopy. When utilizing remote sensing data to drive the model, two vegetation indices (VIs), i.e., normalized difference vegetation index (NDVI) and simple ratio (SR), are combined to calculate FPAR [6], [11]. Although the combination of these two VIs can reflect the vegetation

Manuscript received 7 June 2023; revised 4 September 2023 and 10 October 2023; accepted 14 October 2023. Date of publication 18 October 2023; date of current version 17 November 2023. This work was supported in part by the National Natural Science Foundation of China under Grant 41971305, in part by the Carbon Peak and Carbon Neutrality Innovation Project of Xuzhou under Grant KC23079, in part by the China Europe Dragon 5 Cooperation Programme under Grant 59197, in part by the Double carbon project of Jiangsu Normal University under Grant JSNUSTZX202202, and in part by the Project Funded by the Priority Academic Program Development of Jiangsu Higher Education Institutions under Grant PAPD0705. *(Corresponding author: Liang Liang.)*

The authors are with the College of Geography Surveying and Urban-Rural Planning, Jiangsu Normal University, Xuzhou 221000, China (e-mail: liang_rs@jsnu.edu.cn; wqj1114@163.com; qiusiyi@jsnu.edu.cn; 15190665389@163.com; swang@jsnu.edu.cn).

Digital Object Identifier 10.1109/JSTARS.2023.3325774

cover and reduce the influence of interference factors such as the underlying surface, it is unable to characterize the canopy structure and leaf spatial distribution of vegetation accurately [12]. In fact, the spatial distribution of plant leaves in nature is not completely random, showing a certain degree of aggregation at different scales, which will affect the absorption of light radiation by leaves. To correct the influence of nonrandomness of leaf distribution, Nilson et al. [13] introduced the adjustment parameter Ω in the expression of canopy porosity to characterize the vegetation canopy structure and spatial distribution. Chen and Black [14] called this parameter the clumping index (CI). The CI describes the deviation degree between the real spatial distribution of leaves and the random distribution in the ideal state, which has an impact on plant photosynthesis [15], [16], [17], [18]. In view of this, this study plans to embed the CI in the calculation of FPAR to enable the CASA model to better describe the distribution and structure characteristics of the vegetation canopy to improve the accuracy of NPP estimation.

R_h refers to heterotrophic respiration of soil and is another key parameter used to calculate NEP [19]. R_h can be obtained by direct ground sampling and spatial interpolation [20]. However, for China, a country with a vast territory and diverse ecosystems, the cost of obtaining enough sampling points to ensure the accuracy of spatial interpolation is prohibitive [21]. R_h also can be obtained by constructing an empirical model between R_h ground observations and environmental factors (e.g., humidity and temperature) [20]. However, because the dominant environmental factors affecting R_h in various geographical regions are different, the approach is only adapted to estimate R_h in small-scale homogeneous areas, and it will become unreliable if it is applied to large-scale regions with high spatial heterogeneity [22]. The other approach is indirect estimation, that is, first estimating the soil respiration (R_s) and then utilizing the R_s–R_h model (i.e., the relationship model between R_s and R_h) to obtain R_h [23]. R_s can be obtained through the geostatistical model of soil respiration (GSMSR). The GSMSR is a relatively mature model that has been widely used in large-scale R_s estimation due to its good parameterization methods [24], [25]. Therefore, in this work, the GSMSR model will be used to calculate R_s, and then the R_s–R_h model will be used to obtain R_h of Chinese terrestrial ecosystem.

In this study, using meteorological, remote sensing, and flux station-observed data, we improve the estimation accuracy of Chinese NEP as follows: 1) Using land classification data to optimize the ε_{max} of the CASA model; 2) Using the CI to improve the FPAR enables the model to better describe the characteristics of vegetation canopy structure and leaf spatial distribution; 3) Utilizing the soil respiration models (including R_s–R_h and GSMSR model) to obtain NEP in China and using flux observation data for validation.

II. Study Area and Data

A. Study Area and Observation Stations

China has a vast territory, and complex climate types and landforms form complex terrestrial ecosystems, resulting in spatial differences in carbon sources and sinks in different geographical regions [3], [26]. According to landform and climate, China can be divided into four geographical regions: with the Qinling–Huaihe as the geographic and climatic dividing line, it is divided into the southern and northern region; with the Greater Khingan Mountains–Yinshan Mountains–Helan Mountains as the dividing line, it is divided into the northern and northwestern region; with the Kunlun Mountains–Qilian Mountains–Hengduan Mountains as the dividing line, the Qinghai–Tibet region is separated from the other regions [27], [28] (see Fig. 1).

In this work, the NEP observations of eight eddy covariance flux tower sites, which are publicly available from the ChinaFLUX, are used to verify the model estimation results (see Fig. 1). The eight flux stations are DHS, XSBN, QYZ, CBS, YC, NMG, HB, and DX. Among them, the station DHS and XSBN were covered by evergreen broadleaf forest (EBF), the station QYZ by evergreen needleleaf forest (ENF), the station CBS by deciduous broadleaf forest (DBF), the station YC by cropland, and the stations NMG, HB, and DX by grassland [29], [30]. The eddy related data of the flux tower directly measures the net ecosystem exchange (NEE) observations of carbon dioxide between the atmosphere and ecosystems. After obtaining the NEE value, taking the opposite number can obtain the NEP value for model validation (i.e., NEP $= -$ NEE).

B. Data Sources and Processing

1) Remote Sensing Product Datasets: Remote sensing products include the MODIS vegetation classification dataset (MCD12Q1), MODIS NPP dataset (MOD17A3H v006), NDVI dataset and CI dataset. Among them, the MCD12Q1 and MOD17A3H v006 (500-m resolution) were obtained from the official website of NASA (http://ladsweb.modaps.eosdis.nasa.gov/). The former is used to optimize the model parameter ε_{max}, and the latter is used to validate the model.

The NDVI dataset (1-km resolution) was obtained from the RESDC (i.e., Chinese Resource and Environment Science and Data Center, website: www.resdc.cn). The dataset is produced by the time series data of SPOT/VEGETATION. In this work, the monthly average value of NDVI data of China was calculated using the maximum value synthesis process, which was used to calculate the key parameter FPAR of the CASA model [31].

The CI dataset (500-m resolution) was downloaded from Chinese National Earth System Science Data Center (NESSDC, website: www.geodata.cn). The dataset is calculated based on MODIS albedo products MCD43A1, MCD43A2, and MCD12Q1 [18]. Affected by clouds and other factors, the CI values of some vegetation cover areas are missing. Based on the Python language, we used time series data to linearly interpolate the null value and obtain relatively complete and accurate monthly CI data for China in 2010, which was used to optimize the FPAR. The data were resampled to a 1-km resolution for subsequent analysis.

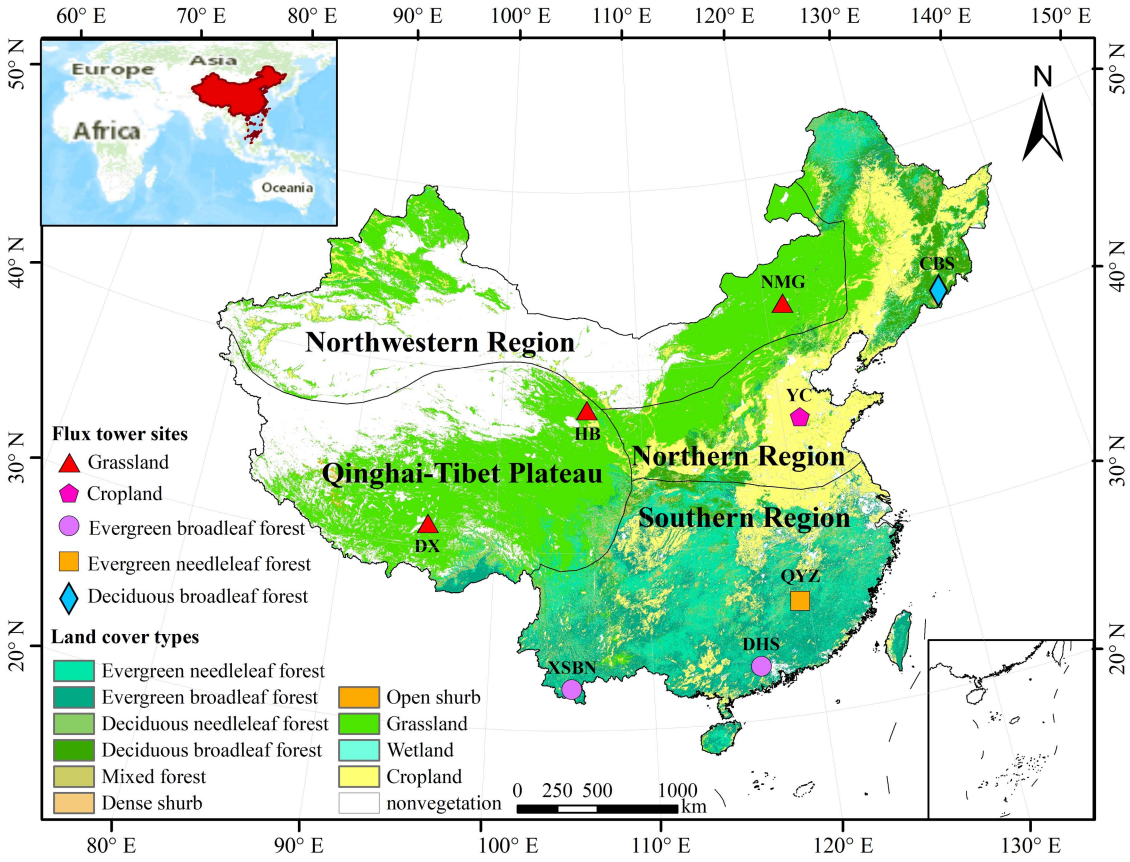

Fig. 1. Land cover types, locations of flux towers sites, and distribution of the four geographical regions.

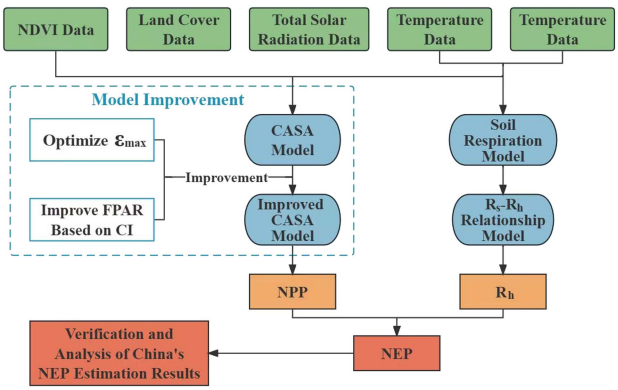

Fig. 2. Flow chart of NEP estimation for terrestrial ecosystems in China.

2) Meteorological Datasets: The monthly average meteorological datasets of China (including the precipitation and temperature data with 1-km resolution) were downloaded from Chinese NESSDC (www.geodata.cn). The dataset was generated by the global 0.5° climate data and its good reliability set has been verified by 496 ground stations [32].

3) DEM Data: The DEM data of China at a 1-km resolution were downloaded from the RESDC (www.resdc.cn). The dataset is applied as an input variable for the total solar radiation value calculation across China.

4) SOCD Data: The soil organic carbon density (SOCD) was the input data of the GSMSR for R_s calculation. Based on previous studies and vegetation classification data, the SOCD values of China's terrestrial ecosystems were set as follows: the value for broadleaf forest is $4.700\,\mathrm{kg}\cdot\mathrm{m}^{-2}$, coniferous forest is $3.770\,\mathrm{kg}\cdot\mathrm{m}^{-2}$, mixed forest is $4.235\,\mathrm{kg}\cdot\mathrm{m}^{-2}$, shrub is $2.560\,\mathrm{kg}\cdot\mathrm{m}^{-2}$, cropland is $2.560\,\mathrm{kg}\cdot\mathrm{m}^{-2}$, and grassland is $1.820\,\mathrm{kg}\cdot\mathrm{m}^{-2}$ [11], [33].

III. Research Methods

A. CASA Model Improvement and NPP Estimation

The original version of CASA model was developed by Potter et al. [9]. The model uses the APAR and $\varepsilon(x,\ t)$ of vegetation to characterize its NPP

$$\mathrm{NPP}(x,\ t) = \mathrm{APAR}(x,\ t) \times \varepsilon(x,\ t) \tag{1}$$

where $\mathrm{APAR}(x,\ t)$ and $\varepsilon(x,\ t)$ are the photosynthetically active radiation absorbed (unit : $\mathrm{MJ}\cdot\mathrm{m}^{-2}\cdot\mathrm{month}^{-1}$) and actual LUE (unit: $\mathrm{gC}\cdot\mathrm{MJ}^{-1}$) of pixel x in month t, respectively. In this article, we will optimize these two parameters for model improvement.

1) FPAR and its Optimization: The APAR absorbed by vegetation can be expressed as follows:

$$\mathrm{APAR}(x,\ t) = 0.5 \times \mathrm{SOL}(x,\ t) \times \mathrm{FPAR}(x,\ t) \tag{2}$$

where $\mathrm{SOL(x,\ t)}$ is the total solar radiation (unit : $\mathrm{MJ \cdot m^{-2} \cdot month^{-1}}$); 0.5 is the ratio coefficient, representing the proportion of effective solar radiation to total solar radiation; FPAR(x, t) refers to the absorption ratio to incident PAR intercepted by vegetation. $\mathrm{SOL(x,\ t)}$ is usually obtained through solar constant, so in expression (2), the accuracy of APAR was determined by FPAR. Two representatives VIs, i.e., SR and NDVI, are utilized to obtain this parameter in the model

$$\mathrm{FPAR\,(x,t)} = \alpha \mathrm{FPAR_{SR}} + (1 - \alpha)\,\mathrm{FPAR_{NDVI}}, \quad (3)$$

where $\alpha = 0.5$ indicates that the calculated results of NDVI and SR account for a weight of 0.5. The expressions of $\mathrm{FPAR_{SR}}$ and $\mathrm{FPAR_{NDVI}}$ are as follows:

$$\mathrm{FPAR_{SR}} = \frac{\mathrm{SR\,(x,\ t)} - \mathrm{SR_{(i,\ min)}}}{\mathrm{SR_{(i,\ max)}} - \mathrm{SR_{(i,\ min)}}} \times (\mathrm{FPAR_{max}} - \mathrm{FPAR_{min}}) + \mathrm{FPAR_{min}} \quad (4)$$

$$\mathrm{SR\,(x,\ t)} = \frac{1 + \mathrm{NDVI(x,\ t)}}{1 - \mathrm{NDVI(x,\ t)}} \quad (5)$$

$$\mathrm{FPAR_{NDVI}} = \frac{\mathrm{NDVI\,(x,\ t)} - \mathrm{NDVI_{(i,min)}}}{\mathrm{NDVI_{(i,\ max)}} - \mathrm{NDVI_{(i,\ min)}}} \times (\mathrm{FPAR_{max}} - \mathrm{FPAR_{min}}) + \mathrm{FPAR_{min}} \quad (6)$$

where $\mathrm{NDVI_{(x,\ t)}}$ and $\mathrm{SR_{(x,\ t)}}$ are the VIs of pixel x in month t; $\mathrm{NDVI_{(i,\ min)}}$, $\mathrm{NDVI_{(i,\ max)}}$, $\mathrm{SR_{(i,\ min)}}$, and $\mathrm{SR_{(i,\ max)}}$ are the maximum and minimum of these VIs for various types of vegetation; $\mathrm{FPAR_{min}}$ and $\mathrm{FPAR_{\ max}}$ take fixed values (0.001 and 0.950, respectively).

In the above methods, the model can obtain good results by combining NDVI and SR to eliminate the deviation caused by a single index. However, there is another problem to be solved: the spatial distribution of leaves between different vegetation types or within the same vegetation type is not completely random but clumps and shows different aggregation characteristics at different levels. These aggregation characteristics can change the radiation environment, have an impact on the photosynthesis of the plant canopy structure, and then affect the productivity of vegetation [15], [16], [17]. The aggregation characteristics of vegetation cannot be reflected through VIs such as NDVI or SR, but rather require CI to characterize. To better express the impact of aggregation effects on photosynthesis, we embed the CI in the FPAR calculation process in the form of a ratio. The expression of the improved FPAR is

$$\mathrm{FPAR\,(x,\ t)} = (0.5 * \mathrm{FPAR_{NDVI}} + 0.5 * \mathrm{FPAR_{SR}}) * \frac{\mathrm{CI\,(x,\ t)}}{\mathrm{CI_{mean\ ref}}} \quad (7)$$

where $\mathrm{CI(x,\ t)}$ is the CI value of pixel x in month t, and $\mathrm{CI_{mean\ ref}}$ is the reference value of various vegetation types. Two schemes will be adopted for the value of $\mathrm{CI_{mean\ ref}}$: one is to use the CI values of different vegetation types obtained from the analysis of global vegetation by He et al. [34] (i.e. scheme I), and the other is to use the mean CI values of different vegetation types counted by the monthly synthetic CI products used in this work (i.e. scheme II). CI is defined as the ratio of the effective leaf area index (LAI) to the true LAI, and its calculation expression is [14]

$$\mathrm{CI} = \mathrm{LAI_e} \ / \ \mathrm{LAI} \quad (8)$$

where $\mathrm{LAI_e}$ is the effective LAI, which can be obtained through the modified Miller equation [14], [18]

$$\mathrm{LAI_e} = -2 \int_0^{\pi/2} \ln\left[P\left(\theta\right)\right] \cos\theta \sin\theta \mathrm{d}\theta. \quad (9)$$

In the process of remote sensing, LAI is an unknown variable, while $\mathrm{LAI_e}$ is a variable derived from porosity using Miller's formula, which is difficult to obtain directly. Therefore, on a large scale, CI data is usually obtained through remote sensing inversion. The CI data used in this study was a dataset produced by Jiao et al. based on MODIS data, and the detailed calculation process can be found in [18].

By analyzing the above expressions, it can be seen that the NDVI and SR data products in (4)–(7) are vegetation index values calculated based on satellite data from specific observation angles, rather than the hemisphere integral values in (9). Therefore, the NDVI and SR indices are difficult to fully reflect the $\mathrm{LAI_e}$, which means it is difficult to fully characterize the ability of vegetation to capture light energy. This study embeds CI into the calculation process of FPAR in the form of a ratio which can effectively correct the deviation caused by solely using VIs (i.e., NDVI and SR) to characterize light energy interception ability. The value of $\frac{\mathrm{CI(x,\ t)}}{\mathrm{CI_{mean\ ref}}}$ will fluctuate around 1. When the ratio is equal to 1, it indicates that the estimated CI is equal to the reference CI, and FPAR remains unchanged. When the ratio is greater than 1, it indicates that the actual estimated CI is greater than the reference CI, the actual aggregation effect is smaller than the reference value, the effective leaf area for photosynthesis is higher, and the actual FPAR should be increased. When the ratio is less than 1, it indicates that the estimated CI is less than the reference value, the actual aggregation effect is greater than the reference value, the effective leaf area is lower, and the FPAR should be reduced.

2) Setting ε_{max} for Different Vegetation Types: $\mathrm{\varepsilon(x,\ t)}$ is another key model parameter. It represents the efficiency of the vegetation in transforming light energy into carbohydrate over a period of time, which is determined by ε_{max}, moisture, and temperature with the following expression:

$$\mathrm{\varepsilon\,(x,\ t)} = \mathrm{W_\varepsilon(x,\ t)} \times \mathrm{T_{\varepsilon 1}(x,\ t)} \times \mathrm{T_{\varepsilon 2}(x,\ t)} \times \varepsilon_{max} \quad (10)$$

where $\mathrm{W_\varepsilon(x,\ t)}$, $\mathrm{T_{\varepsilon 1}(x,\ t)}$, and $\mathrm{T_{\varepsilon 2}(x,\ t)}$ present the effects of water, low temperature, and high temperature stress, respectively. ε_{max} is the vegetation LUE in the optimal growth environment (unit : $\mathrm{gC \cdot MJ^{-1}}$). Parameter ε_{max} is a key parameter and the value is uniformly set to 0.389 in the original version [6], [9]. However, research shows that it is more reasonable to set specific values according to different vegetation types. Referring to previous studies on the ε_{max} of various vegetation types [10], [11], [35], the ε_{max} values are revalued as follows: the ENF is 0.476, the EBF is 0.980, the DNF is 0.485, the DBF is 0.692, the MXF is 0.768, the shrub is 0.429, the grassland and cropland are 0.542, and other vegetation are 0.389. Other parameters

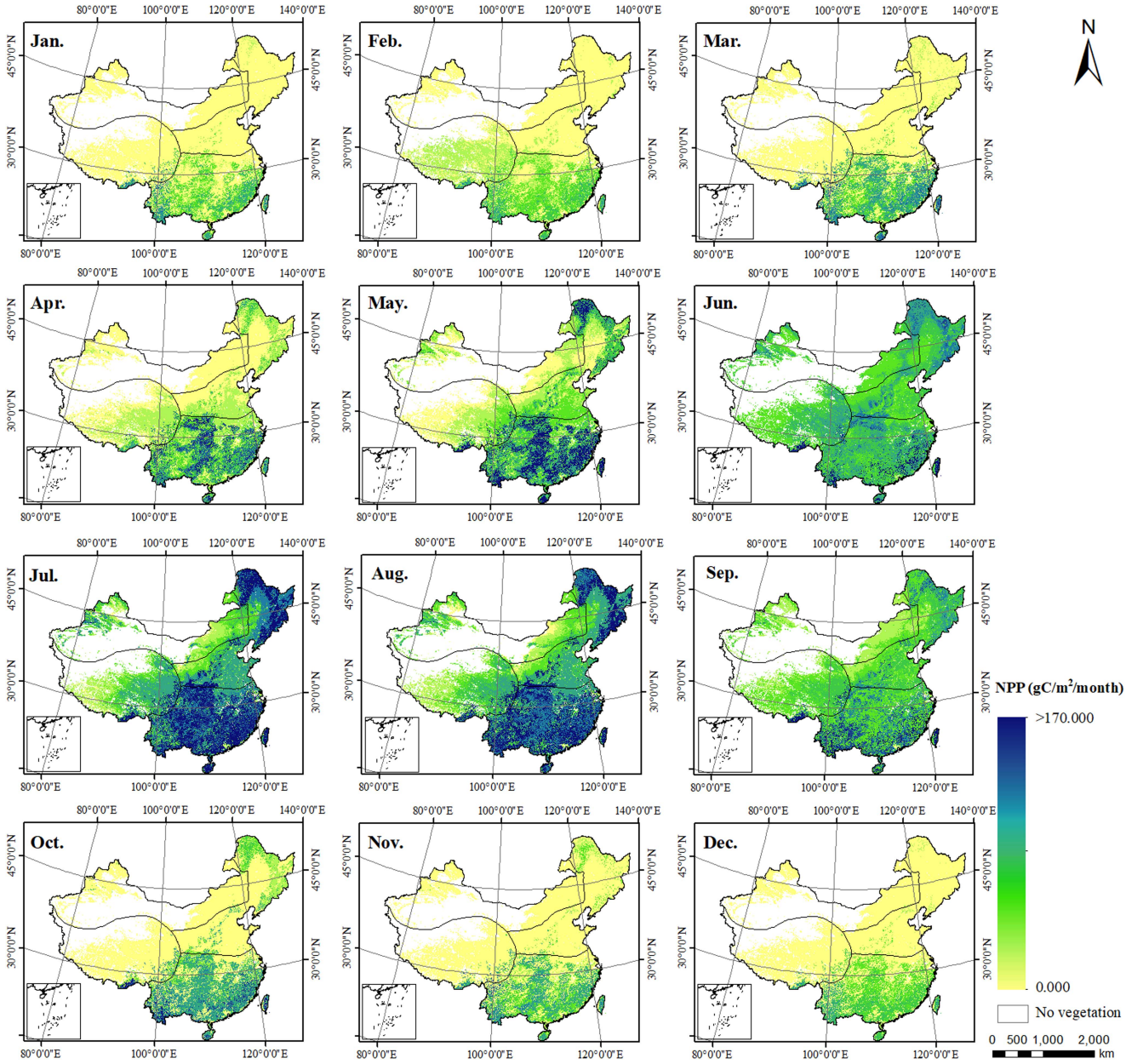

Fig. 3. Spatial pattern of NPP over China during 2010 by the improved CASA model.

in expression (8) are calculated according to the conventional method. For details, please refer to Liang et al. [11].

In the calculation process, we combine the vegetation classification data with the ε_{max} values of various vegetation as the model inputs, so as to obtain the optimized $\varepsilon(x, t)$ value of each pixel for NPP estimations improvement.

B. Estimation of Soil Respiration

1) GSMSR Model and Rs *Estimation:* GSMSR model uses precipitation, temperature, and SOCD as input data to estimate R_s. Yu et al. [25] studied soil respiration using a large number of ground observation validation data and obtained the following expression of monthly soil respiration in China:

$$R_{s,\,monthly} = (R_{D_s=0} + M \times D_s) \times e^{\ln\alpha e^{\beta T} T/10} \times (P + P_0) / (P + K), \quad (11)$$

where $R_{s,\,monthly}$ is the total soil respiration in a month (unit : $gC \cdot m^{-2} \cdot month^{-1}$); $R_{D_s=0}$ is the average monthly soil respiration when SOCD is 0, with a fitting value of 0.588 (unit : $gC \cdot m^{-2} \cdot month^{-1}$); D_s is the SOCD of soil in the depth range of 0–20 cm, and its coefficient M is taken as 0.188; α and β take the fitted values of 1.830 and 0.006, respectively; T and P are the monthly mean temperature (unit : °C) and total precipitation in a month (unit : cm), respectively; and K takes a fixed value

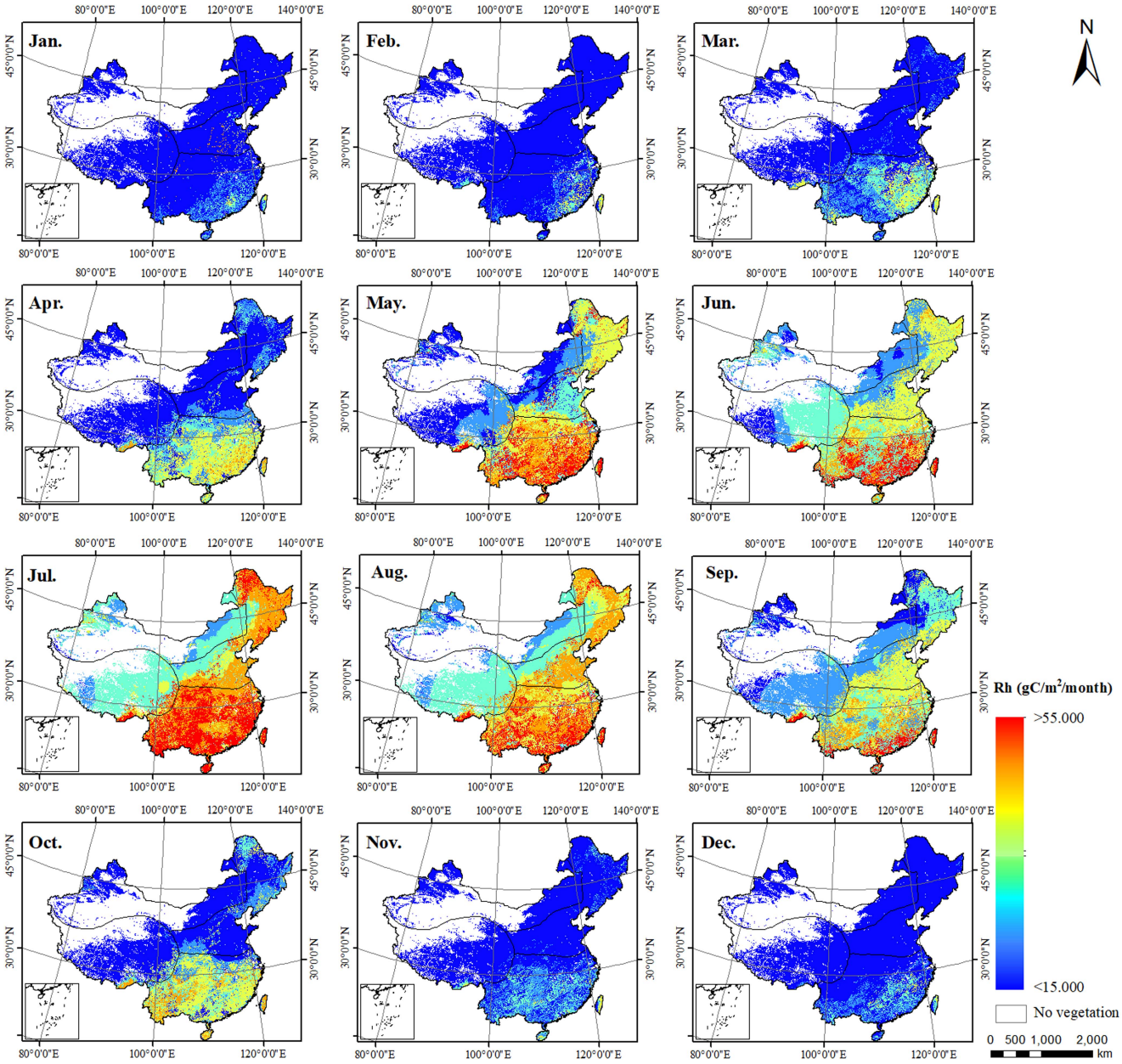

Fig. 4. Spatial pattern of R_h over China during 2010 by the GSMSR and R_s–R_h model.

of 5.657. For the detailed derivation process of expression (11), please refer to [25].

2) Rs–Rh *Relationship Model and Rh Estimation:* R_s can be obtained by using the GSMSR model; however, R_h is required in the estimation of NEP. Shi et al. established the R_s–R_h relationship model by using R_s and R_h observations in various periods and places of China [23], [25]:

$$\mathrm{R_h} = -0.0009\mathrm{R_s^2} + 0.6011\mathrm{R_s} + 4.8874 \qquad (12)$$

where R_s and R_h are the monthly respiration and heterotrophic respiration of soil, respectively (unit : $\mathrm{gC \cdot m^{-2} \cdot month^{-1}}$).

C. Ground Observation Data Acquisition and Model Accuracy Verification

The ground observations were obtained from the China FLUX to verify the NEP estimations. The data were preprocessed and quality controlled according to the ChinaFLUX technical system standardization (for details, please refer to [36], [37]). In addition, among the released ground observation data, the data in 2010 are relatively complete, so we used the data of that year for verification.

Based on the coordinate position of each flux station, the NEP of the pixel (1 km $\times$ 1 km) with the corresponding points on the NEP thematic map is extracted and compared with the station observation value. The root mean square errors (RMSEs)

TABLE I
COMPARISON OF VARIOUS TYPES OF VEGETATION ANNUAL NPP ($gC \cdot M^{-2} \cdot A^{-1}$) BETWEEN MOD17A3H AND OPTIMIZED MODEL

Vegetation types	Reference NPP (MOD17A3H)	CASA Model optimized by ε_{max}		CASA Model optimized by CI (scheme I)		CASA Model optimized by CI (scheme II)	
	NPP values	NPP values	Percentage Deviation	NPP values	Percentage Deviation	NPP values	Percentage Deviation
ENF	705.367	701.637	-0.529	948.90	34.526	702.70	-0.378
EBF	767.051	811.981	5.857	893.00	16.420	801.80	4.530
DNF	477.025	340.510	-28.618	352.70	-26.063	339.20	-28.893
DBF	565.624	516.450	-8.694	495.70	-12.362	513.50	-9.215
MXF	700.982	525.496	-25.034	530.10	-24.378	524.00	-25.248
Shrub	332.307	366.007	10.141	317.00	-4.606	369.20	11.102
grassland	198.50	183.444	-7.585	182.50	-8.060	180.00	-9.320
cropland	416.00	270.829	-34.897	273.60	-34.231	269.00	-35.337

and coefficient of determination (R^2) are used as indicators for accuracy verification of each model.

The overall process of estimating NEP in China's terrestrial ecosystem was shown in Fig. 2.

IV. RESULTS AND ANALYSIS

A. NPP Estimation and Analysis of China

1) NPP Estimation: The NPP was estimated by utilizing the CASA model (including optimized and original version). Fig. 3 is the NPP estimations of the China's terrestrial ecosystem using the CASA model optimized by scheme II. Due to the vast territory, the NPP spatial-temporal distribution of China varies. In terms of temporal variation, the monthly NPP gradually increases from spring to summer, reaching its peak in July and August, and gradually decreases from autumn to winter.

In terms of spatial variation, NPP shows marked zonal characteristics, and the change trend gradually decreases from southeast to northwest, showing the distribution pattern south > north > Qinghai –Tibet > north. This is related to water, heat, and light conditions, as well as vegetation types. In the longitudinal direction, the distribution of water resources in China gradually decreases from east to west; in the latitudinal direction, the solar radiation gradually weakens from south to north. Therefore, due to the appropriate temperature and abundant precipitation, the vegetation in the south grows rapidly, with the maximum NPP value of 630.127 $gC \cdot m^{-2} \cdot a^{-1}$. The northwest and Qinghai–Tibet are dominated by arid and alpine regions, with relatively sparse vegetation and slow growth, resulting in low NPP values (255.780 and 170.287 $gC \cdot m^{-2} \cdot a^{-1}$, respectively). In the northern region, the temperature is lower than that in the south, and rainfall is more abundant than that in the Qinghai–Tibet and northwest, so the NPP is lower than that in the south but higher than that in other regions, with a mean value of 324.565 $gC \cdot m^{-2} \cdot a^{-1}$. In addition, the NPP values of the various vegetation are different (The order is EBF > ENF > DBF > DNF). The vegetation in the south is mainly EBF and ENF, and the NPP value in most areas is above 700.00 $gC \cdot m^{-2} \cdot a^{-1}$, so the value in this region is high; the northwest and Qinghai–Tibet are dominated by grassland, and the NPP value in most areas is below 180.00 $gC \cdot m^{-2} \cdot a^{-1}$, so the value is relatively low.

2) Analysis of NPP Estimations: The reliability of the estimated NPP is verified with MOD17A3H data. MOD17A3H is a widely used NPP dataset provided by NASA's EOS/MODIS, but it can only obtain annual products. We synthesized the annual NPP value through the results of monthly estimates and compared it with MOD17A3H (Table I).

Table I shows the NPP of various types of vegetation based on MOD17A3H and the CASA model optimized by different methods. The NPP values of EBF and ENF estimated by the CASA model optimized by the CI (scheme I) are abnormally higher than others, indicating that this scheme may overestimate NPP.

The estimation results of the other two methods are relatively consistent. The percentage deviation of ENF, EBF, DBF, and grassland was relatively small, with deviations below 0.529%, 5.857%, 9.215%, and 9.357%, respectively, while the deviation of cropland was relatively large (approximately 35.00%). This may be because the Biome-BGC model used for producing MOD17A3H lacks a module to estimate carbon flux of cropland, so it is difficult to accurately estimate cropland NPP. In addition, crop growth is greatly affected by irrigation, fertilization, and other anthropogenic factors, which further leads to great uncertainty in NPP.

B. NEP Estimation and Validation of China

1) Estimation of R_h *in China:* Fig. 4 shows the monthly R_h in China. R_h depends on the microbial community in the soil. Therefore, similar to the NPP, R_h in China is also

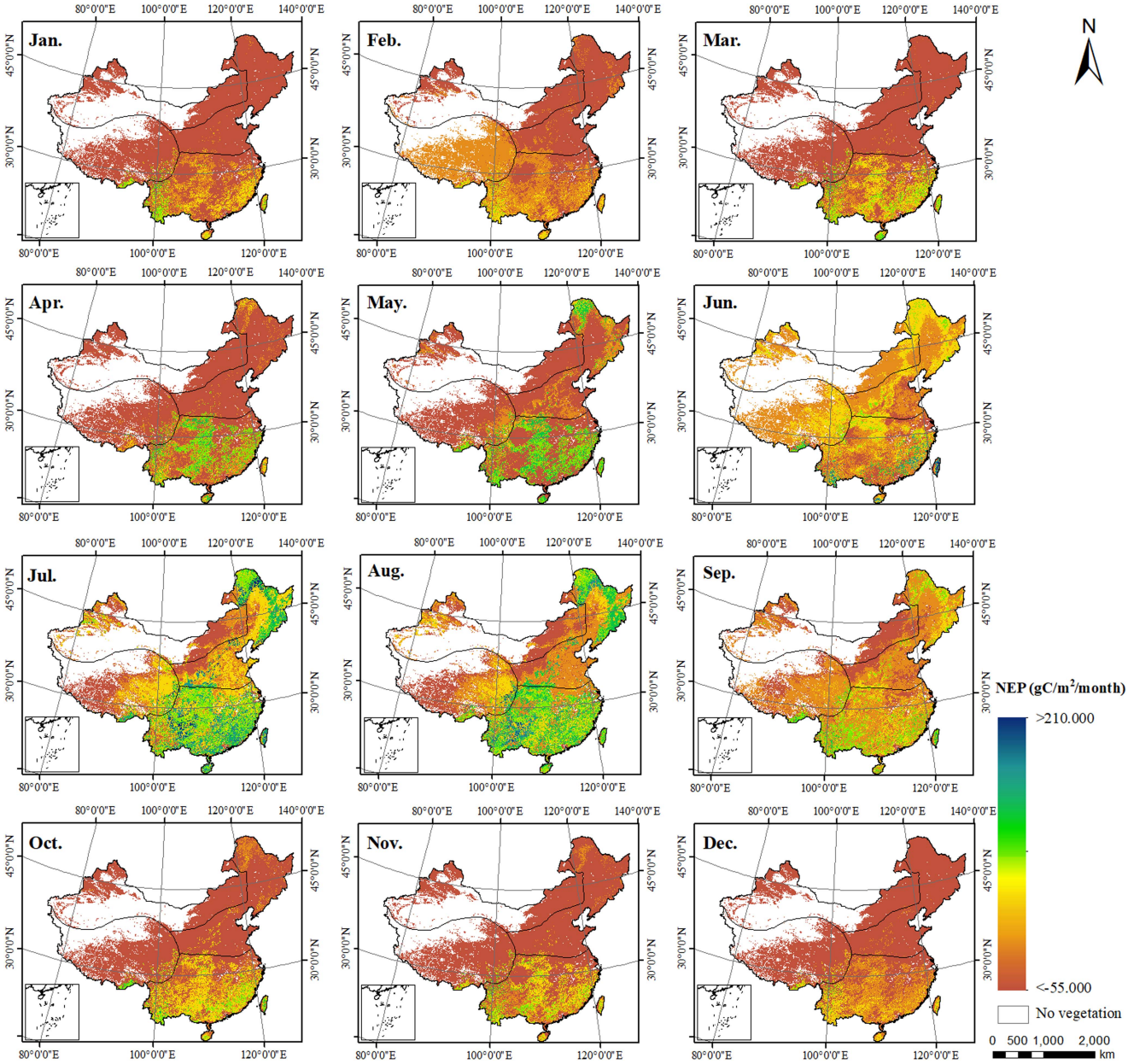

Fig. 5. Spatial pattern of NEP over China during 2010 by the CASA model and soil respiration model.

affected by precipitation and temperature. Spatially, R_h is relatively high in the southeast and low in the northwest and the values of the four geographical regions followed the order south (409.887 $gC \cdot m^{-2} \cdot a^{-1}$) > north (303.972 $gC \cdot m^{-2} \cdot a^{-1}$) > Qinghai–Tibet (251.845 $gC \cdot m^{-2} \cdot a^{-1}$) > northwest (233.036 $gC \cdot m^{-2} \cdot a^{-1}$). In terms of time, R_h gradually increases from spring to summer, reaching its peak in August (38.220 $gC \cdot m^{-2} \cdot month^{-1}$), and gradually decreases from autumn to winter.

2) Monthly Variation of NEP in China: Fig. 5 shows the NEP estimations of China, which is calculated by using the NPP based on the model optimized by the CI (see scheme II). The Spatiotemporal distribution of NEP in China is similar to that of NPP. In general, the China's NEP value of each month gradually decreases from southeast to northwest, and its variation during the year is a single-peak curve [see Figs. 5 and 6(a)]. The curve increased sharply from May, peaked at 30.758 $gC \cdot m^{-2} \cdot month^{-1}$ in July, then decreased, and dropped to a trough of -4.585 $gC \cdot m^{-2} \cdot month^{-1}$ in December. Overall, according to the estimation of the improved model, the annual NEP value of China's terrestrial ecosystem in 2010 was approximately 0.235 $Pg \cdot year^{-1}$.

The temporal changes of NEP are inconsistent in the different regions [see Fig. 6(b)]. The values of different regions are in the order south > north > Qinghai–Tibet > northwest. Among them, the NEP value of the southern in each month is positive (the annual value reaches 220.240 $gC \cdot m^{-2} \cdot a^{-1}$), while that of the northern and Qinghai–Tibet are positive

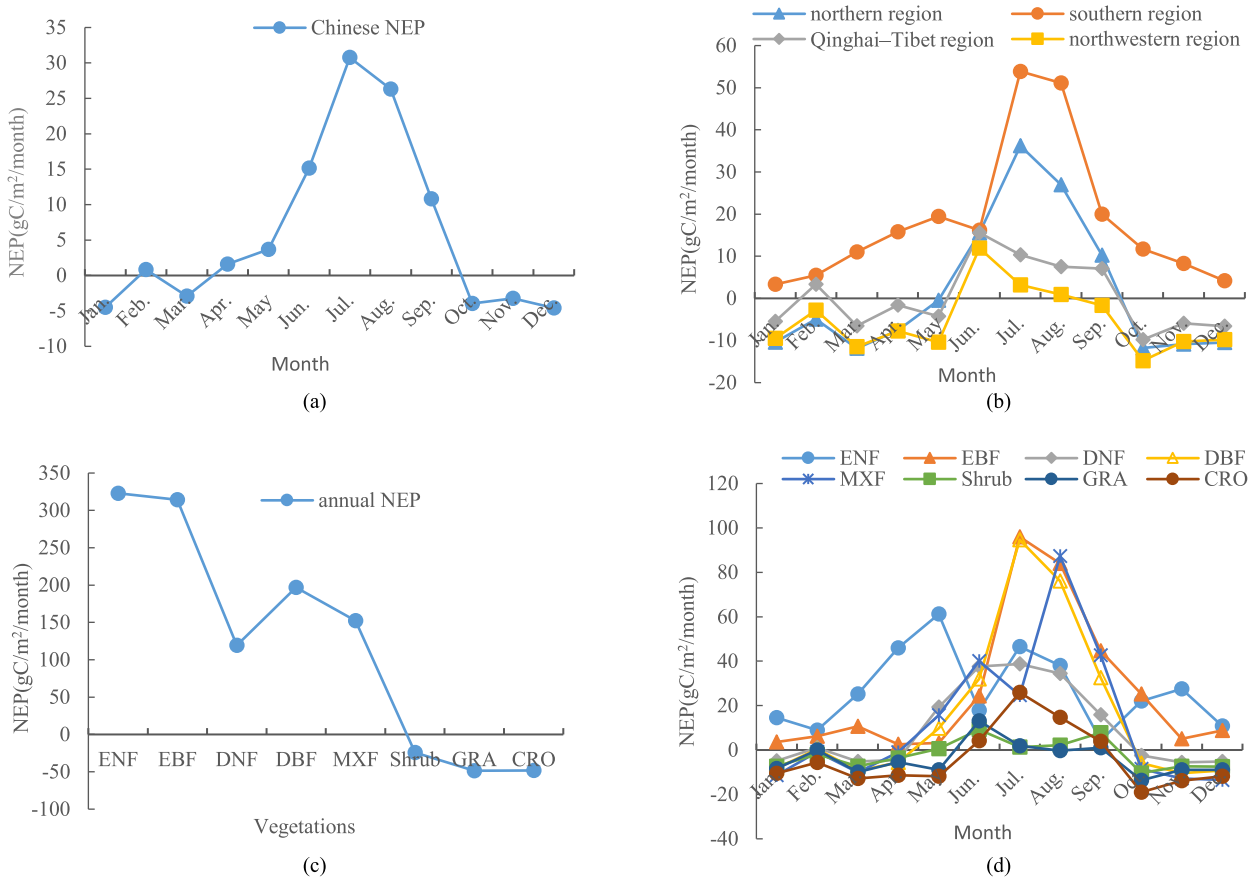

Fig. 6. Annual analysis results of NEP in China. (a) Monthly average NEP of the whole country. (b) Monthly average NEP of different regions. (c) Annual NEP of each vegetation type. (d) Monthly average NEP of each vegetation type.

from June to September (the annual values are 20.593 and 3.751 gC · m^{-2} · a^{-1}, respectively). For the whole year, these three regions are shown as carbon sinks. The NEP values of the northwestern regions in most months of the year are negative (the annual value is −62.250 gC · m^{-2} · a^{-1}), and for the whole year, this region is shown as a carbon sources. In addition, the values of the Qinghai–Tibet and northwest peaked in June, while that of the south and north peaked in July.

The seasonal variation of NEP differs among various types of vegetation [see Fig. 6(c) and (d)]. The values of EBF and ENF are greater than zero in each season, indicating that these forests are carbon sinks throughout the year. Other vegetation, such as DNF, DBF, MXF, shrubs, grasslands and farmland, are carbon sinks in summer and carbon sources in spring and winter. The annual NEP of DNF, DBF, MXF and shrubs is greater than 0, indicating that they are carbon sinks overall in a year; shrub, farmland, and grassland are overall carbon sources in a year, with annual values of −24.436, −48.568, −48.568, and –48.147 gC · m^{-2} · a^{-1}, respectively [see Fig. 6(c)].

3) Validation of Simulated NEP: According to the GPS information of the observation points, the station-observed NEP values and estimated NEP values of the original version CASA model [see Fig. 7(a)] and optimized CASA model with different improvement schemes [see Fig. 7(b)–(d)] were matched and comparatively analyzed. Then, the accuracy of each model was evaluated according to the RMSEs and R^2.

Fig. 7(a) and (b) shows that using different ε_{max} values for different vegetation can effectively optimize the results. Compared to the original version, the estimation accuracy of the optimized model that adopted the vegetation classification of the ε_{max} parameter was higher, as indicated by the RMSE value decrease from 21.139 to 12.024 gC · m^{-2} · $month^{-1}$ and the R^2 value increase from 0.413 to 0.775.

Optimizing the model with CI data can further improve the result. The figure shows that the estimation accuracy is improved after using the two schemes to improve the FPAR [see Fig. 7(b)–(d)]. Using the optimal model of scheme I, the indicator R^2 is improved from 0.775 to 0.794, but the RMSE value is also slightly increased from 12.024 to 14.183 gC · m^{-2} · $month^{-1}$. The reason is that the estimations of the optimal model with scheme I have a better correlation with the observed value but generally overestimate the NEP values, so the RMSE increases slightly. This corresponds to the analysis result of NPP in the previous text (see Table I). The model improved by scheme II has the highest accuracy, indicated by the RMSE decreasing to 10.179 gC · m^{-2} · $month^{-1}$ and the R^2 increasing to 0.832, which is the preferred scheme for NEP estimation.

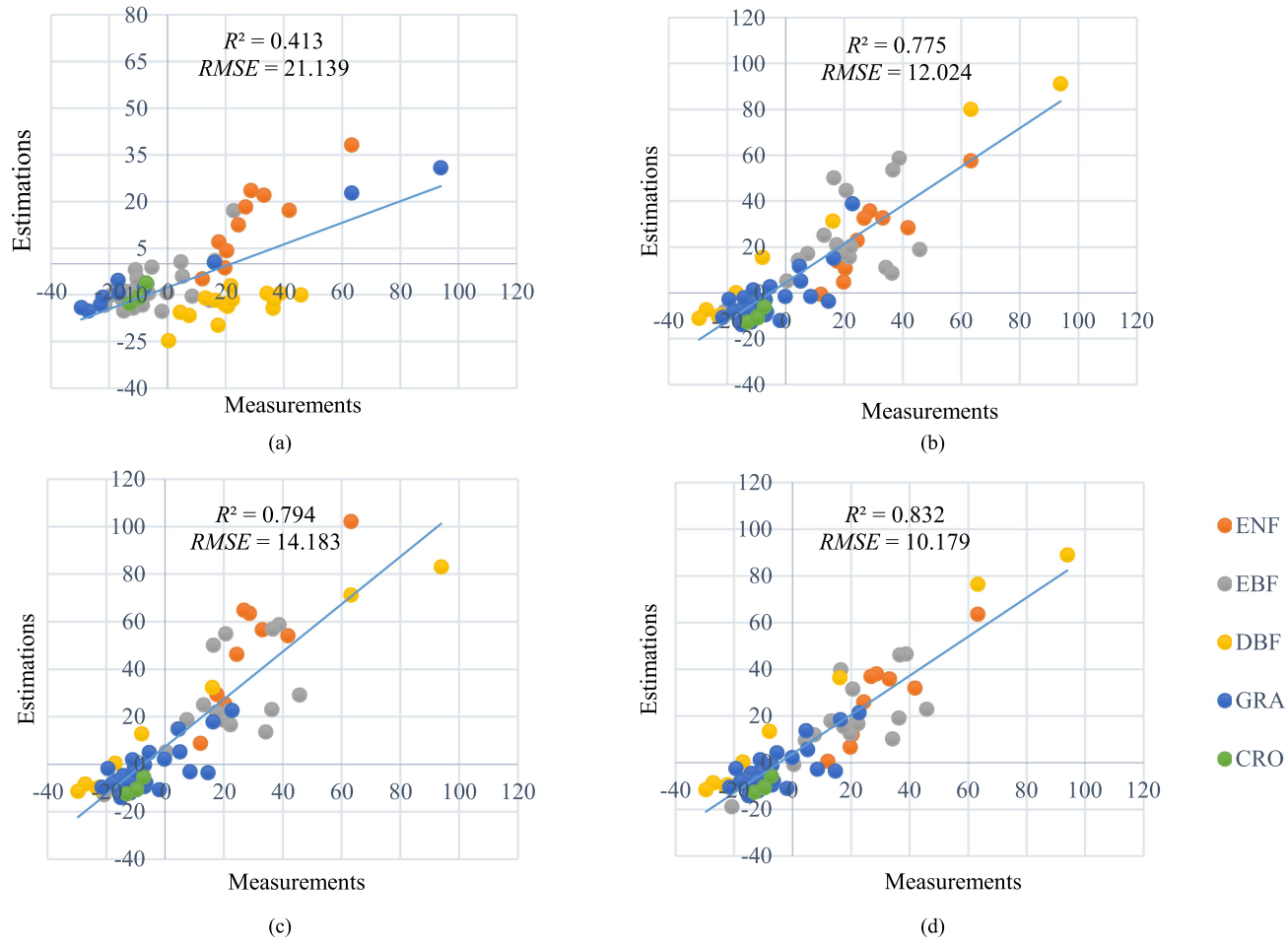

Fig. 7. Observed NEP versus. estimated NEP ($gC \cdot m^{-2} \cdot month^{-1}$) based on the CASA model. (a) ε_{max} with fixed value of 0.389 ($gC \cdot MJ^{-1}$). (b) ε_{max} using vegetation classification. (c) ε_{max} using vegetation classification + adopting scheme I to embed the CI. (d) ε_{max} using vegetation classification + adopting scheme II to embed the CI.

V. Discussion

A. Optimization of ε_{max} With Classification Data

The value of ε_{max} was set to 0.389 $gC \cdot MJ^{-1}$ for different vegetation in the CASA model's original version [9]. Nevertheless, in fact, ε_{max} is a parameter characterizing the vegetation photosynthetic potential, and various kinds of vegetation have different ε_{max} due to their leaf shape, canopy structure, and photosynthetic capacity. Research shows that the value of ε_{max} can be taken between 0.09 $gC \cdot MJ^{-1}$ and 2.16 $gC \cdot MJ^{-1}$ [10]. In this work, ε_{max} was determined according to vegetation classification data and the research of Zhu et al. [10], [11], [34]. The results show that the optimization of ε_{max} can effectively correct the underestimation of NPP in the China's terrestrial ecosystem, which is more reasonable than the range estimated by the original CASA model, indicating that ε_{max} optimization is an important approach to improve the NPP estimations.

B. Optimization of FPAR With the CI Dataset

The CI characterizes the leaf aggregation degree of the vegetation canopy and is an important structural parameter that affects canopy radiation transmission [16], [17]. The ε_{max} of various vegetation types are different, and the canopy structure and spatial distribution also show different clustering characteristics within the same vegetation type, affected by regional, environmental, soil, and other factors. Most leaves are clustered in natural conditions (CI<1) and show different degrees of aggregation on various scales [38], [39]. The stronger the aggregation effect of leaves is, the lower the CI, and the closer its value is to 0. In contrast, the lower the aggregation effect is, the higher the CI, and the value is close to 1. In the original CASA model, the NDVI and SR were combined to calculate FPAR. Although this strategy can better characterize vegetation cover and vegetation growth status and eliminate some radiation errors, it is still difficult to characterize the aggregation effect within the vegetation [12], [40]. The study of Chen et al. [16] shows that when CI is not considered, the gross primary productivity (GPP) will be underestimated. To overcome this problem, the CI is embedded into the CASA model in the form of a ratio, which represents well the internal heterogeneity of various vegetation types, thus improving the estimation of NEP (see Fig. 7). The results indicated that using the CI to optimize FPAR is another effective method to improve the CASA model.

This study adopted two different schemes to embed the CI into the model. In scheme I, the denominator $\mathrm{CI}_{\mathrm{mean\ ref}}$ in the correction term $\frac{\mathrm{CI}(x,\,t)}{\mathrm{CI}_{\mathrm{mean\ ref}}}$ adopts the research results of He et al. [34]. In this scheme, $\mathrm{CI}_{\mathrm{mean\ ref}}$ is the annual average value processed by the Ross–Li model based on the MODIS BRDF product (MCD43A1), while the CI dataset used in the scheme II was calculated in this study (Global MODIS monthly synthetic dataset). There are differences between the two processing methods. Therefore, although the R^2 of NPP estimation has increased, there is an overestimation in vegetation types such as ENF and EBF, resulting in a high RMSE value. The numerator and denominator terms of scheme II are calculated based on MODIS monthly synthetic data. They underwent the same preprocessing method and have less error, so better results are obtained. In addition, the denominator $\mathrm{CI}_{\mathrm{mean\ ref}}$ of scheme II is the monthly average value, which has a higher time resolution than the annual average value of scheme I and can reflect the monthly variation in vegetation, which is another important reason for scheme II achieving better results.

C. NEP Estimations of the Coupled Model

NPP, which can be directly estimated by CASA model, is the focus of most studies [41], [42], [43], [44]. However, after estimating NPP, R_h must be subtracted in order to calculate the NEP value that can characterize vegetation carbon sinks. [2], [4], [44]. Thus, in this article, the NPP and R_h are estimated and then the NEP in China is calculated on this basis.

The NEP of China's terrestrial ecosystem generally decreases from southeast to northwest and presents a single-peak curve with a peak in July and a valley in December. The above results have strong correlations with the spatial distribution and temporal changes in precipitation and temperature, indicating that hydrothermal conditions are likely to be the main factor affecting NEP across China [45].

In this work, the optimized CASA model was coupled with the R_s–R_h and GSMSR model for NEP estimation in different regions of China. It can provide support for the analysis of regional carbon sources and sinks in China and the formulation of regional carbon balance policies. In the next step, we will use higher spatial resolution data to produce long-time series NEP products and analyze in depth the NEP change trend in China and its relationship with climate, human activities, and other factors.

VI. Conclusion

NEP is a critical indicator of the ecosystem carbon cycle. To estimate NEP accurately, the CASA model was improved by using the land classification data to set the $\varepsilon_{\max}$ with various types of vegetation more reasonably and introducing the CI to describe the canopy structure and vegetation distribution more accurately. Then, the R_h was estimated by combining the R_s–R_h and GSMSR model and the NEP of China, which can characterize carbon sinks, was obtained. The main conclusions of this study are as follows:

1) Optimizing parameter $\varepsilon_{\max}$ is an effective approach for CASA model improvement. Compared with the original model, the improved model with $\varepsilon_{\max}$ values set based on different vegetation has more accurate estimation results. It can be seen that studying the photosynthetic potential of various vegetation types in different regions and accurately obtaining their $\varepsilon_{\max}$ values is a key step in improving the accuracy of NEP estimation in terrestrial ecosystems.
2) Using the CI to optimize FPAR is another feasible method to improve the CASA model. The research indicates that embedding CI in FPAR calculations in the form of ratios can better characterize the canopy structure and spatial distribution characteristics of vegetation, thereby improving estimation accuracy. This result provides a new way to effectively utilize CI datasets.
3) Due to the factors such as hydrothermal conditions and vegetation types, the NEP values in China exhibit a decreasing distribution pattern from southeast (warm and humid areas) to northwest (cold and arid areas). The NEP values in different regions of China are in the order of South > North > Qinghai–Tibet > Northwest, and the monthly variation of NEP in each region shows a unimodal curve and reaches its peak in summer.

Acknowledgment

The authors would like to thank the data provided by National Earth System Science Data Center and National Geographic Resource Science SubCenter.

References

[1] K. Pathak, Y. Malhi, G. W. Sileshi, A. K. Das, and A. J. Nath, "Net ecosystem productivity and carbon dynamics of the traditionally managed Imperata grasslands of North East India," *Sci. Total Environ.*, vol. 635, pp. 1124–1131, Sep. 2018, doi: 10.1016/j.scitotenv.2018.04.230.

[2] Y. T. Yao et al., "A new estimation of China's net ecosystem productivity based on eddy covariance measurements and a model tree ensemble approach," *Agricultural Forest Meteorol.*, vol. 253/254, pp. 84–93, May 2018, doi: 10.1016/j.agrformet.2018.02.007.

[3] M. Zhang, X. J. Huang, X. W. Chuai, X. L. Xie, Z. Y. Zhu, and Y. Wang, "Spatial distribution and changing trends of net ecosystem productivity in China," *Geography Geo-Inf. Sci.*, vol. 36, no. 2, pp. 69–74, Mar. 2020.

[4] O. Goncharova, G. Matyshak, M. Udovenko, O. Semenyuk, H. Epstein, and A. Bobrik, "Temporal dynamics, drivers, and components of soil respiration in urban forest ecosystems," *Catena*, vol. 185, pp. 104299–104299, Feb. 2020, doi: 10.1016/j.catena.2019.104299.

[5] G. R. Yu et al., "High carbon dioxide uptake by subtropical forest ecosystems in the East Asian monsoon region," *Proc. Nat. Acad. Sci. USA*, vol. 111, no. 13, pp. 4910–4915, Apr. 2014, doi: 10.1073/pnas.1317065111.

[6] C. B. Field, M. J. Behrenfeld, J. T. Randerson, and P. Falkowski, "Primary production of the biosphere: Integrating terrestrial and oceanic components," *Science*, vol. 281, no. 5374, pp. 237–240, Jul. 1998, doi: 10.1126/science.281.5374.237.

[7] J. Wang, C. Y. Wu, X. Y. Wang, and X. Y. Zhang, "A new algorithm for the estimation of leaf unfolding date using MODIS data over China's terrestrial ecosystems," *Int. Soc. Photogrammetry Remote Sens. J. Photogrammetry Remote Sens.*, vol. 149, pp. 77–90, Mar. 2019, doi: 10.1016/j.isprsjprs.2019.01.017.

[8] H. Z. Sun et al., "Relationships between climate change, phenology, edaphic factors, and net primary productivity across the Tibetan Plateau," *Int. J. Appl. Earth Observ. Geoinf.*, vol. 107, 2022, Art. no. 102708, doi: 10.1016/j.jag.2022.102708.

[9] C. S. Potter et al., "Terrestrial ecosystem production: A process model based on global satellite and surface data," *Glob. Biogeochem. Cycles*, vol. 7, no. 4, pp. 811–841, Dec. 1993, doi: 10.1029/93gb02725.

[10] W. Q. Zhu, Y. Z. Pan, H. He, D. Y. Yu, and H. B. Hu, "Simulation of maximum light utilization of typical Chinese vegetation," *Chin. Sci. Bull.*, vol. 51, pp. 700–706, Mar. 2006.

[11] L. Liang et al., "Remote sensing estimation and spatiotemporal pattern analysis of terrestrial net ecosystem productivity in China," *Remote Sens.*, vol. 14, no. 8, pp. 1–23, Apr. 2022, doi: 10.3390/rs14081902.
[12] L. Liang et al., "Estimation of crop LAI using hyperspectral vegetation indices and a hybrid inversion method," *Remote Sens. Environ.*, vol. 165, no. 8, pp. 123–134, May 2015, doi: 10.1016/j.rse.2015.04.032.
[13] T. Nilson, "A theoretical analysis of the frequency of gaps in plant stands," *Agricultural Meteorol.*, vol. 8, pp. 25–38, Jan. 1971, doi: 10.1016/0002-1571(71)90092-6.
[14] J. M. Chen and T. A. Black, "Defining leaf area index for non-flat leaves," *Plant Cell Environ.*, vol. 15, no. 4, pp. 421–429, May 1992, doi: 10.1111/j.1365-3040.1992.tb00992.x.
[15] J. M. Chen, J. Liu, S. G. Leblanc, R. Lacaze, and J. L. Roujean, "Multi-angular optical remote sensing for assessing vegetation structure and carbon absorption," *Remote Sens. Environ.*, vol. 84, no. 4, pp. 516–525, Jun. 2003, doi: 10.1016/S0034-4257(02)00150-5.
[16] J. M. Chen et al., "Effects of foliage clumping on the estimation of global terrestrial gross primary productivity," *Glob. Biogeochem. Cycles*, vol. 26, no. 1, Jan. 2012, Art. no. GB1019, doi: 10.1029/2010GB003996.
[17] G. Zhu, W. Ju, J. M. Chen, P. Gong, B. Xing, and J. Zhu, "Foliage clumping index over China's landmass retrieved from the MODIS BRDF parameters product," *IEEE Trans. Geosci. Remote Sens.*, vol. 50, no. 6, pp. 2122–2137, Jan. 2012.
[18] Z. Jiao et al., "An algorithm for the retrieval of the clumping index (CI) from the MODIS BRDF product using an adjusted version of the kernel-driven BRDF model," *Remote Sens. Environ.*, vol. 209, pp. 594–611, Mar. 2018.
[19] R. Brown and D. Markewitz, "Soil heterotrophic respiration: Measuring and modeling seasonal variation and silvicultural impacts," *Forest Ecol. Manage.*, vol. 430, pp. 594–608, Dec. 2018, doi: 10.1016/j.foreco.2018.08.018.
[20] J. Q. Li, E. Pendall, F. A. Dijkstra, and M. Nie, "Root effects on the temperature sensitivity of soil respiration depend on climatic condition and ecosystem type," *Soil Tillage Res.*, vol. 199, May 2020, Art. no. 104574, doi: 10.1016/j.still.2020.104574.
[21] X. G. Wang et al., "Dissecting soil CO_2 fluxes from a subtropical forest in China by integrating field measurements with a modeling approach," *Geoderma*, vol. 161, no. 1, pp. 88–94, Jun. 2010, doi: 10.1016/j.geoderma.2010.12.010.
[22] W. Xie, S. T. Chen, and Z. H. Hu, "Factors influencing the variability in soil heterotrophic respiration from terrestrial ecosystem in China," *Environ. Sci.*, vol. 35, no. 1, pp. 334–340, Jan. 2014.
[23] Z. H. Shi, "Spatial-temporal simulation of vegetation carbon sink and its influential factors based on CASA and GSMSR model in Shaan Xi province," Ph.D. dissertation, Northwest A&F Univ., Shaanxi, China, 2015.
[24] B. Bond-Lamberty, C. K. Wang, and S. T. Gower, "A global relationship between the heterotrophic and autotrophic components of soil respiration?," *Glob. Change Biol.*, vol. 10, no. 10, pp. 1756–1766, Jan. 2004, doi: 10.1111/j.1365-2486.2004.00816.x.
[25] G. R. Yu et al., "Spatiotemporal pattern of soil respiration of terrestrial ecosystems in China: The development of a geostatistical model and its simulation," *Environ. Sci. Technol.*, vol. 44, no. 16, pp. 6074–6080, Aug. 2010, doi: 10.1021/es100979s.
[26] F. X. Gu et al., "Climate-driven uncertainties in modeling terrestrial ecosystem net primary productivity in China," *Agricultural Forest Meteorol.*, vol. 246, pp. 123–132, Nov. 2017, doi: 10.1016/j.agrformet.2017.06.011.
[27] L. Liang et al., "Long-term spatial and temporal variations of vegetative drought based on vegetation condition index in China," *Ecosphere*, vol. 8, no. 8, Aug. 2017, Art. no. e01919, doi: 10.1002/ecs2.1919.
[28] Z. E. Niu et al., "An increasing trend in the ratio of transpiration to total terrestrial evapotranspiration in China from 1982 to 2015 caused by greening and warming," *Agricultural Forest Meteorol.*, vol. 279, Feb. 2018, Art. no. 107701, doi: 10.1016/j.agrformet.2019.107701.
[29] G. R. Yu, X. F. Wen, X. M. Sun, B. D. Tanner, X. Lee, and J. Y. Chen, "Overview of ChinaFLUX and evaluation of its eddy covariance measurement," *Agricultural Forest Meteorol.*, vol. 137, no. 3/4, pp. 125–137, Apr. 2006, doi: 10.1016/j.agrformet.2006.02.011.
[30] X. Chai et al., "Carbon flux phenology and net ecosystem productivity simulated by a bioclimatic index in an alpine steppe-meadow on the Tibetan Plateau," *Ecol. Model*, vol. 394, pp. 66–75, Feb. 2019, doi: 10.1016/j.ecolmodel.2018.12.024.
[31] X. Xu, "China monthly vegetation index (NDVI) spatial distribution dataset," 2018. [Online]. Available: https://www.resdc.cn/data.aspx?DATAID=343
[32] S. Z. Peng, Y. X. Ding, W. Z. Liu, and Z. Li, "1 km monthly temperature and precipitation dataset for China from 1901 to 2017," *Earth Syst. Sci. Data*, vol. 11, no. 4, pp. 1931–1946, Dec. 2019, doi: 10.5194/essd-11-1931-2019.
[33] X. L. Xie, "Study on soil organic carbon stocks in national and regional scale using GIS," Ph.D. dissertation, Nanjing Normal Univ., Nanjing, China, 2004.
[34] L. M. He, J. M. Chen, J. Pisek, C. B. Schaaf, and A. H. Strahler, "Global clumping index map derived from the MODIS BRDF product," *Remote Sens. Environ.*, vol. 119, pp. 118–130, Jun. 2012, doi: 10.1016/j.rse.2011.12.008.
[35] D. Y. Yu, P. J. Shi, H. B. Shao, W. Q. Zhu, and Y. Z. Pan, "Modelling net primary productivity of terrestrial ecosystems in East Asia based on an improved CASA ecosystem model," *Int. J. Remote Sens.*, vol. 30, no. 18, pp. 4851–4866, Jun. 2009, doi: 10.1080/01431160802680552.
[36] K. Wilson et al., "Energy balance closure at FLUXNET sites," *Agricultural Forest Meteorol.*, vol. 113, no. 1, pp. 223–243, Jun. 2002, doi: 10.1016/S0168-1923(02)00109-0.
[37] T. L. R. O. Foken, "Corrections and data quality," in *Eddy Covariance: A Practical Guide to Measurement and Data Analysis*, M. Aubinet, T. Vesala, and D. Papale, Eds., Berlin, Germany: Springer-Verlag, 2012.
[38] G. L. Zhu, "Spatial-temporal characteristics of foliage clumping index in China during 2000–2013," *Chin. Sci. Bull.*, vol. 61, no. 14, pp. 1595–1603, May 2016, doi: 10.1360/n972015-00987.
[39] S. S. Wei, H. L. Fang, C. B. Schaaf, L. M. He, and J. M. Chen, "Global 500 m clumping index product derived from MODIS BRDF data (2001–2017)," *Remote Sens. Environ.*, vol. 232, pp. 111296–111296, Oct. 2019, doi: 10.1016/j.rse.2019.111296.
[40] L. Liang et al., "Estimation of leaf nitrogen content in wheat using new hyperspectral indices and a random forest regression algorithm," *Remote Sens.*, vol. 10, no. 12, Dec. 2018, Art. no. 1940, doi: 10.3390/rs10121940.
[41] K. Tan, S. Y. Zhou, E. Z. Li, and P. J. Du, "Assessing the impact of urbanization on net primary productivity using multi-scale remote sensing data: A case study of Xuzhou, China," *Front. Earth Sci.*, vol. 9, no. 2, pp. 319–329, Jun. 2015, doi: 10.1007/s11707-014-0454-7.
[42] Q. Wang et al., "Insights into spatiotemporal variations in the NPP of terrestrial vegetation in Africa from 1981 to 2018," *Remote Sens.*, vol. 15, no. 11, May 2023, Art. no. 2748, doi: 10.3390/rs15112748.
[43] W. H. Zhao et al., "Estimation of the net primary productivity of winter wheat based on the near-infrared radiance of vegetation," *Sci. Total Environ.*, vol. 838, May 2018, Art. no. 156090, doi: 10.1016/j.scitotenv.2022.156090.
[44] S. Qiu et al., "Estimation of European terrestrial ecosystem NEP based on an improved CASA model," *IEEE J. Sel. Topics Appl. Earth Observ. Remote Sens.*, vol. 16, no. 1, pp. 1244–1255, Dec. 2023, doi: 10.1109/JSTARS.2022.3233128.
[45] Y. Wang et al., "Precipitation-use efficiency may explain net primary productivity allocation under different precipitation conditions across global grassland ecosystems," *Glob. Ecol. Conservation*, vol. 20, Oct. 2019, Art. no. e00713, doi: 10.1016/j.gecco. 2019.e00713.

Liang Liang received the Ph.D. degree in photogrammetry and remote sensing from Central South University, Changsha, China, in 2010.

He is currently an Associate Professor with Jiangsu Normal University, Xuzhou, China. He has engaged in remote sensing research for over ten years and authored or coauthored more than 60 publications in *Environmental Remote Sensing*, *International Journal of Remote Sensing* and other journals. His current research is mainly on vegetation parameter inversion and NEP estimation based on remote sensing data and its applications in agriculture and environment.

Qianjie Wang received the bachelor's degree in remote sensing science and technology from the School of Geography, Geomatics and Planning, Jiangsu Normal University, Xuzhou, China, in 2021. She is currently working toward the master's degree in photogrammetry and remote sensing with Jiangsu Normal University.

Her research interest is urban carbon sink research.

Siyi Qiu received the master's degree in photogrammetry and remote sensing from the School of Geography, Geomatics and Planning, Jiangsu Normal University, Xuzhou, China, in 2022.

Her research interests include ecological remote sensing and carbon sink research.

Di Geng received the master's degree in photogrammetry and remote sensing from the School of Geography, Geomatics and Planning, Jiangsu Normal University, Xuzhou, China, in 2021.

Her research interests include carbon sink model research and carbon sink research.

Shuguo Wang received the B.S. degree in photogrammetry and remote sensing from Wuhan University, Wuhan, China, in 2003, and the Ph.D. degree in cartography and geography information system from the Graduate University of Chinese Academy of Sciences, Beijing, China, in 2010.

Since 2014, he has been with the School of Geography, Geomatics and Planning, Jiangsu Normal University, Xuzhou, China. His research interests include microwave remote sensing, estimation of soil moisture by multisource observation data, and related validation issues.